ISSN 1060-992X, Optical Memory and Neural Networks, 2017, Vol. 26, No. 4, pp. 249–256. © Allerton Press, Inc., 2017.

3D Crystal Structure Identification Using Fuzzy Neural Networks

D. V. Kirsh[a, b, *], O. P. Soldatova[a], A. V. Kupriyanov[a, b], I. A. Lyozin[a], and I. V. Lyozina[a]

[a] *Samara National Research University, Samara, 443086 Russia*

[b] *Image Processing Systems Institute—Branch of the Federal Scientific Research Centre "Crystallography and Photonics" of the Russian Academy of Sciences, Samara, 443001 Russia*

**e-mail: kirshdv@gmail.com*

Received July 10, 2017; in final form, September 5, 2017

Abstract—The problem of recognizing nano-scale images of lattice projections comes down to identification of crystal lattice structure. The paper considers two types of fuzzy neural networks that can be used for tackling the problem at hand: the Takagi-Sugeno-Kang model and Mamdani-Zadeh model (the latter being a modification of the Wang-Mendel fuzzy neural network). We offer a three-stage neural network learning process. In the first two stages crystal lattices are grouped in non-overlapping classes, and lattices belonging to overlapping classes are recognized at the third stage. In the research, we thoroughly investigate the applicability of the neural net models to structure identification of 3D crystal lattices.

Keywords: crystal lattice, fuzzy neural networks, crystal structure identification, lattice system, unit cell, Takagi-Sugeno-Kang neural network, Wang-Mendel neural network

DOI: 10.3103/S1060992X17040026

INTRODUCTION

Being the fundamental concept of crystallography and having Angstrom-order sizes, Bravais lattices are building blocks for all crystals. Every crystal is constructed of these lattices in various modifications. At the same time, different crystals can have the same lattices. There is a total of 14 such lattices. Depending on special symmetry, all crystals are distributed among seven lattice systems: triclinic, monoclinic, tetragonal, orthorhombic, trigonal, hexagonal, and cubic systems [1]. Figure 1 presents the general arrangements of Bravais lattices (smallest structural cells) for each lattice system.

The type of a lattice system is determined by six parameters of a Bravais lattice: the lengths of the three edges and three angles between them (see Table 1).

The task of recognizing nano-scale images, which are projections of crystal lattices, can be reduced to the structure identification problem. Among basic lattice structure identification methods are: the comparator of the National Institute of Standards and Technology [2], packing efficiency-based identification [3] and isosurface-based identification [4].

Table 1. Parameters of Bravais unit cells of basic lattice systems

Name	Lengths of edges	Values of angles
Triclinic (*aP*)	$l_1 \neq l_2 \neq l_3$	$\alpha_1 \neq \alpha_2 \neq \alpha_3$
Monoclinic (*mP*)	$l_1 \neq l_2 \neq l_3$	$\alpha_1 = \alpha_2 = 90^\circ \neq \alpha_3$
Trigonal (*hR*)	$l_1 = l_2 = l_3$	$\alpha_1 = \alpha_2 = \alpha_3 \neq 90^\circ$
Hexagonal (*hP*)	$l_1 = l_2 \neq l_3$	$\alpha_1 = 120^\circ; \alpha_2 = \alpha_3 = 90^\circ$
Orthorhombic (*oP*)	$l_1 \neq l_2 \neq l_3$	$\alpha_1 = \alpha_2 = \alpha_3 = 90^\circ$
Tetragonal (*tP*)	$l_1 = l_2 \neq l_3$	$\alpha_1 = \alpha_2 = \alpha_3 = 90^\circ$
Cubic (*cP*)	$l_1 = l_2 = l_3$	$\alpha_1 = \alpha_2 = \alpha_3 = 90^\circ$

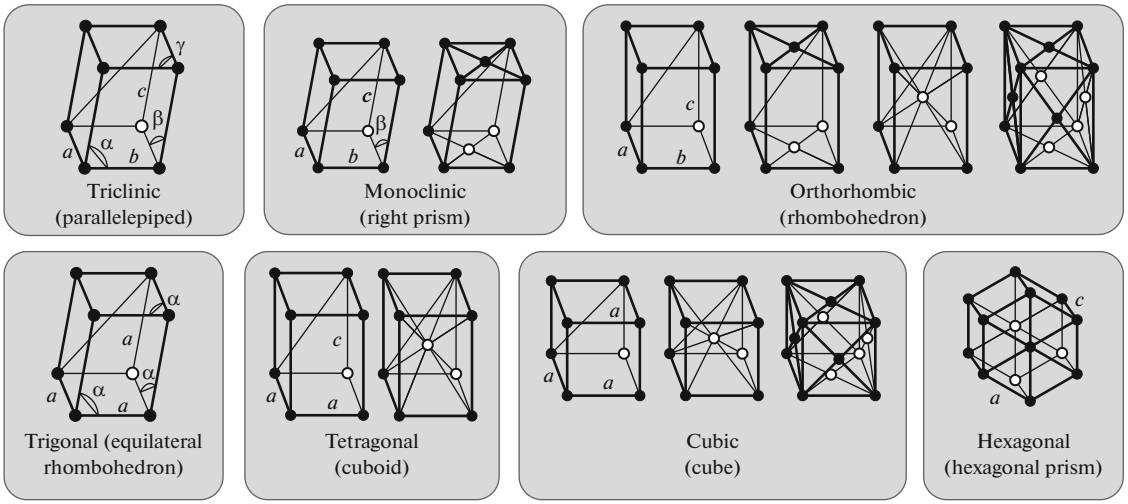

Fig. 1. The unit cells of seven lattice systems.

However, these approaches have some drawbacks that restrict their use: the tricky process of crystal preparation (the need for accurate polishing and mounting), low efficiency of comparison of similar lattices, high sensitivity to minor distortions of lattice node coordinates.

The major difficulty here is the ambiguity in choosing a two-dimensional basic cell for a particular projection (Fig. 2) [5].

Papers [6, 7] give a careful investigation of this problem representing a Bravais lattice as a unique feature space allowing the resolution of any nano-scale images in elementary structures.

One of possible approaches to the determination of crystal lattice type is offered in [8] where previously estimated lattice parameters are compared with predefined reference lattice parameters. The lattice is considered to belong to a particular type if its parameters have the closest match with the parameters of the reference lattice of this type.

Another solution to the problem is given in paper [9]. The relationship between the number of equal distances and inter-particle distances and angles of observation in the projection of the lattice is used to classify a Bravais lattice. A classifier consisting of 15 neural nets, which allow for all possible pairwise permutations of elementary Bravais lattices, is offered for classification of Bravais lattices. Each network can recognize two classes. The result of the classification is a class that receives the greatest number of votes in pair comparison. The architecture with two hidden layers and a sigmoidal activation function is taken for each of the neural networks.

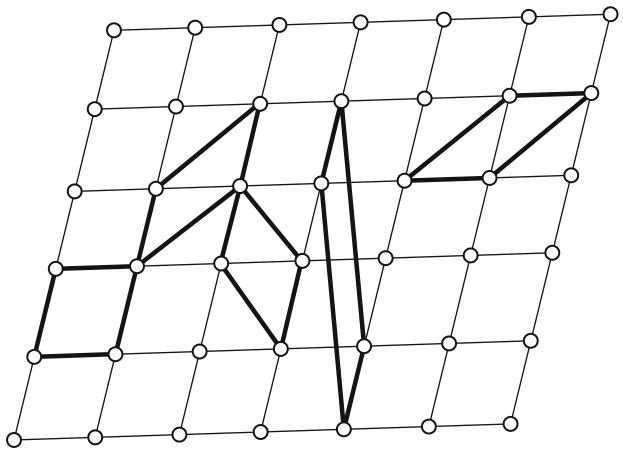

Fig. 2. The choice set for a two-dimensional basic cell.

Since the classes of Bravais lattices are overlapping, our idea is to use fuzzy neural networks. This kind of networks combines learning and generalization abilities of neural nets, fuzzy logic operations (which allow us to determine the degree of class inclusion of an object as a real number from 0 to 1), and possibility to classify fuzzy rule-oriented bases. A class with the highest degree of class inclusion is the result of structure identification.

The determination of classification parameters from experimental results and expert evaluation of the parameters are the most popular classification methods using fuzzy neural nets. Research works [10–15] consider this kind of neural networks for solving classification problems using experimental results. Particularly, the author of paper [15] modifies Takagi-Sugeno-Kang (TSK) neural network by introducing the recurrent TSK net. The trick

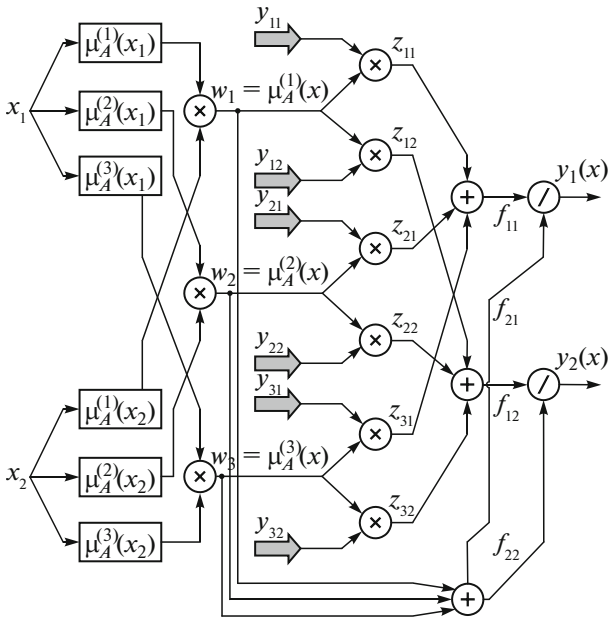

Fig. 3. The structure of fuzzy TSK neural network with two inputs, three inference rules and two outputs.

allows the automatic generation of fuzzy rules, but increases the computational complexity of the learning algorithm. Paper [16] proposes a fuzzy TSK neural network for tackling the classification problem. The net uses the expert evaluation method to choose the most informative classification features and form fuzzy inference rules. In paper [17] similar approaches are used for learning the author's modification of the Wang-Mendel network. The drawback of the method is the use of subjective estimations of fairly large number of experts and necessity to evaluate their consistency.

Conventional fuzzy rule-based neural net models and modified TSK and Wang-Mendel networks use the algebraic product or minimum-form logical product as a fuzzy Boolean conjunction. Respectively, these models use algebraic sum or maximum-form Boolean sum as a fuzzy Boolean disjunction [15, 17–19]. At the same time research [20] allows a conclusion about the effective use of fuzzy logical operations used in algebras of Goedel, Goguen and Lukasiewicz. Paper [21] offers and investigates modifications of Wang-Mendel networks that allows us to operate fuzzy logical operations defined in these algebras.

The fuzzy TSK neural network model and Wang-Mendel network modification (Mamdani-Zadeh networks using operations of Goedel algebra) have been investigated using samples of 700 and 7000 parameter sets of Bravais lattices belonging to 7 lattice system classes.

FUZZY NETWORKS MODELS

Figure 3 shows an example of fuzzy TSK multiple-output neural network.

Generalized Gauss function

$$\mu_A(x_j) = \frac{1}{1 + \left(\dfrac{x_j - c_j}{\sigma_j}\right)^{2b_j}} \tag{1}$$

is used as a fuzzification function for each variable x_j.

The fuzzy conjunction in the form of algebraic product

$$\mu_A^{(i)}(x) = \prod_{j=1}^{N} \left[1 \Big/ \left(1 + \left(\frac{x_j - c_j^{(i)}}{\sigma_j^{(i)}} \right)^{2b_j^{(i)}} \right) \right], \tag{2}$$

is used to aggregate the condition of the i-th rule.

Given M inference rules, the aggregation of the network output is done by formula (3), which can be represented as

$$y(x) = \frac{1}{\sum\limits_{i=1}^{M} w_i} \sum_{i=1}^{M} w_i y_i(x), \tag{3}$$

where $y_i(x) = p_{i0} + \sum_{j=1}^{N} p_{ij} x_j$ is the aggregation of implication. Weights w_i in this expression are interpreted as components $\mu_A^{(i)}(x)$ defined by (2).

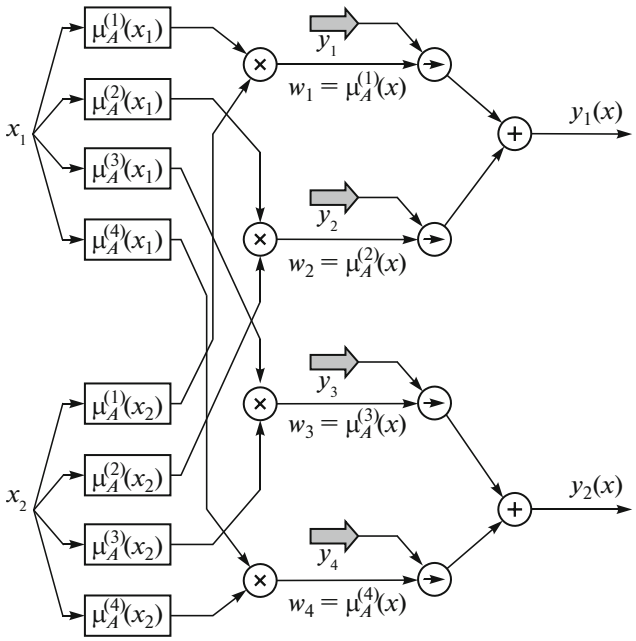

Fig. 4. The structure of fuzzy Mamdani-Zadeh inference neural network with two inputs, four inference rules and two outputs.

The first layer of the network is responsible for fuzzification of each variable $x_j\,(j = 1,2,\ldots,N)$ defining the coefficient of belonging $\mu_A^{(i)}(x_j)$ for each i-th inference rule according to the fuzzification function used. This is a parametric layer whose parameters $\left(c_j^{(i)},\sigma_j^{(i)},b_j^{(i)}\right)$ are subject to adaptation in learning.

The second layer makes aggregation of particular variables x_j defining the resulting coefficient of belonging $w_i = \mu_A^{(i)}(x)$ in accordance with formula (2). The third layer is the TSK function generator that calculates $y_i(x) = p_{i0} + \sum_{j=1}^{N} p_{ij}x_j$. In addition, this layer computes the products of signals $y_i(x)$ and weights w_i found in the previous layer. This is a parametric layer with adaptable linear weights p_{ij} $(i = 1,2,\ldots,M; j = 1,2,\ldots,N)$.

The forth layer has two neuron-adders, one of which calculates the weighed sum of signals $y_i(x)$, and the other sums up the weights $\sum_{i=1}^{M} w_i$.

The fifth layer consists of several output neurons. This is a normalizing layer where the weights are normalized according to (3). Output signals $y_s(x)$ are defined as

$$y_s(x) = f_s(x) = \frac{f_{1s}}{f_{2s}}. \tag{4}$$

An instance of the structure of Mamdani-Zadeh network, which is a modification of popular Wang-Mendel network, is shown in Fig. 4.

This is a four-layer structure where the first layer is similar to that of the TSK network. The second layer performs pairwise aggregation of particular variables x_j defining the resulting coefficient of belonging $w_i = \mu_A^{(i)}(x)$ for vector x in accordance with formula (5) – the fuzzy conjunction as minimum. This is not a parametric layer.

$$w_i = \mu_A^{(i)}(x_k) \otimes \mu_A^{(k)}(x_k) = \min\left\{\mu_A^{(i)}(x_k),\mu_A^{(k)}(x_k)\right\}. \tag{5}$$

The third layer is responsible for fuzzy implication in accordance with formula (6) in which variables v_i stand for conclusion of inference rules formed in the process of learning. This is a parametric layer.

$$\mu_{A\to B}(w_i,v_i) = \begin{cases} 1, & w_i \le v_i \\ v_i, & w_i > v_i \end{cases}. \tag{6}$$

The forth layer consists of some output neurons which realize the fuzzy disjunction operation as maximum (7) where variables z_i and z_k are the results of implication the i-th and k-th rules of inference.

$$z_i \oplus z_k = \max\{z_i, z_k\}. \tag{7}$$

THE LEARNING TECHNIQUE

The data of generated unit cells of 7 different types were used for learning the neural networks. The data were generated using the crystal lattice modeling method described in [22, 23] under the following conditions:

(1) The number of lattices per each lattice system is 100 and 1000.

(2) The minimum admissible difference between "unequal" cell edges is 0.050 angst;

Table 2. Instance of file arrangement holding lattice cell parameters for various lattice systems

l_1^2	l_2^2	l_3^2	$2l_2l_3\cos\alpha_1$	$2l_1l_3\cos\alpha_2$	$2l_1l_2\cos\alpha_3$
15.417	6.500	8.780	0	0	1.429
13.301	13.301	1.447	13.301	0	0
15.417	6.775	8.780	0	0	1.429
22.243	12.462	3.224	0	0	0
19.193	19.193	19.193	15.583	15.583	15.583
15.506	8.734	6.428	5.871	0.342	2.438

Table 3. Grouping of lattice system types

Lattice system type	l_1^2	l_2^2	l_3^2	$2l_2l_3\cos\alpha_1$	$2l_1l_3\cos\alpha_2$	$2l_1l_2\cos\alpha_3$	Subgroup no.
Triclinic (*aP*)	x	x	x	x	x	x	1
Trigonal (*hR*)	x	x	x	x	x	x	1
Hexagonal (*hP*)	x	x	x	x	0	0	2
Monoclinic (*mP*)	x	x	x	0	0	x	3
Orthorhombic (*oP*)	x	x	x	0	0	0	4
Tetragonal (*tP*)	x	x	x	0	0	0	4
Cubic (*cP*)	x	x	x	0	0	0	4

(3) The minimum admissible difference between "unequal" cell angles is 0.02 rad;

(4) The maximum admissible difference between the reference and estimated values of cell edges is 0.010 angst;

(5) The maximum admissible difference between the reference and estimated values of cell angles is 0.010 rad.

The parameters of unit cell generation are:

(1) The minimum edge lengths are 1.000 angst, 1.000 angst, 1.000 angst;

(2) The maximum edge lengths are 5.000 angst, 5.000 angst, 5.000 angst;

(3) The minimum angle values 0.175 rad, 0.175 rad, 0.175 rad;

(4) The maximum angle values 1.571 rad, 1.571 rad, 1.571 rad.

The size of lattice in each direction was taken equal to three nodes. The G6-space notation [24] was used to bring the parameters of unit cells to a common value range. The data files holding parameters of generated cells are arranged as shown in Table 2.

The preliminary examination of original data allowed us to divide 7 lattice types in 4 groups according to the quantity and ordinal numbers of non-zero columns in data files. The grouping of crystal lattices is given in Table 3.

After that the TSK and Mamdani-Zadeh neural nets were subjected to learning and tested in three stages:

(1) Pair training and testing of neural nets for recognition of 2 lattice types;

(2) Training and testing of neural nets for recognition of all 7 lattice types;

(3) Training and testing of neural nets for recognition of lattice types in subgroups 1 and 4.

DETERMINING THE CRYSTAL LATTICE TYPE

The relative error of structure identification in all experiments was calculated as a percentage of identification failures over the whole test lattice collection. At the first stage 6-dimensional vectors comprising of learning data of two types were fed to the TSK and Mamdani-Zadeh neural nets. The output layer held two neurons according to the number of classes being recognized. The results are similar for both network models (see Tables 4 and 5).

Table 4. Relative errors of crystal lattice structure identification in pair learning of the TSK network using a 700-lattice sample

	hR (1)	*hP* (2)	*mP* (3)	*oP* (4)	*tP* (4)	*cP* (4)
Triclinic (*aP*)	0	0	1	1	0	0
Trigonal (*hR*)		0	2	0	0	0
Hexagonal (*hP*)			0	0	0	0
Monoclinic (*mP*)				4	2	0
Orthorhombic (*oP*)					12	2
Tetragonal (*tP*)						6

Table 5. Relative errors of crystal lattice structure identification in pair learning of the TSK network using a 7000-lattice sample

	hR (1)	*hP* (2)	*mP* (3)	*oP* (4)	*tP* (4)	*cP* (4)
Triclinic (*aP*)	10	0	0	0	1	1
Trigonal (*hR*)		0	0	0	0	2
Hexagonal (*hP*)			15	15	43	12
Monoclinic (*mP*)				42	16	10
Orthorhombic (*oP*)					16	8
Tetragonal (*tP*)						12

Better identification results for the 700-lattice sample can be explained by the insufficient size of the learning sample: the chance of finding two similar (in the terms of G6 parameters) lattices becomes lower with the decreasing size of the learning sample. For this reason, the largest sample of 7000 lattices looks preferable.

It is also worth noticing that the neural nets could not discriminate triclinic lattices (in fact, arbitrary lattices) from trigonal lattices (three equal edges and three equal angles). The reason is that the placing of these two lattice types in a single subgroup is not entirely correct: triclinic lattices are described by six independent parameters (six non-zero columns), and trigonal lattices by two independent parameters (also six non-zero columns). So, we put these two lattice types in one subgroup "formally" rather than "physically".

Let us compare our results with the classification of crystal lattices into three groups according to the number of equal translations and inter-translation angles given in paper [9]. The neural nets discriminate low-ranking lattice types (triclinic and trigonal lattices) quite readily (the identification failure rate is 10%).

The middle-ranking lattice types (hexagonal and monoclinic ones) can also be discriminated quite easily by the both network models (the identification failure rate is 15%). Separating them from high-ranking lattices (tetragonal and orthorhombic types) causes much difficulty (the identification failure rate is over 40%), which naturally follows from the similarity of their edges. The high-ranking lattices themselves (orthorhombic, tetragonal and cubic types) are discerned by the both neural network models quite successfully (the identification failure rate is about 12%).

At the second stage of the investigation, the data collection presenting all the seven lattice types was used to train the both neural nets. Six-dimensional vectors made up of this data were fed to the TSK and Mamdani-Zadeh neural nets. According to the number of classes to be recognized, the output layer had seven neurons. The experimental results show that the both network models recognize hexagonal- and monoclinic-type lattices (subgroups 2 and 3) without failure. It is because the learning data for these lattice types has different combinations of zero and non-zero columns than that for other lattice types. In other words, the neural nets recognize the lattices of hexagonal and monoclinic type as non-overlapping classes.

Additionally, the third stage of experiments was carried out to recognize lattice types belonging to subgroups 1 and 4. The TSK and Mamdani-Zadeh neural nets with 6 inputs and 2 outputs were used to deal with lattices of subgroup 1. The same nets with 3 inputs corresponding to non-zero columns of initial data and 3 outputs were engaged to process subgroup 4. The identification failure rate of the TSK neural net

Table 6. Relative errors of crystal lattice structure identification when using parametric identification methods

	hR (1)	*hP* (2)	*mP* (3)	*oP* (4)	*tP* (4)	*cP* (4)
Triclinic (*aP*)	0	0	1	0	0	0
Trigonal (*hR*)		0	0	2	3	26
Hexagonal (*hP*)			7	0	0	0
Monoclinic (*mP*)				22	10	0
Orthorhombic (*oP*)					34	15
Tetragonal (*tP*)						26

was 6%/10% (in the case of 700/7000 lattice sample, respectively) for subgroup 1, and 18%/25% for subgroup 4. With the Mamdani-Zadeh neural net this rate was 24%/4% for lattices from subgroup 1 and 18%/12% for subgroup 4.

The results confirm the supposition that the amount of 700 lattices is not sufficient for a learning sample. The covering density grows with the size of a learning sample. As a result, a network begins "recognizing" not only non-zero columns, but also the matching of values in columns 1–3 and 4–6 of trigonal lattices.

It is very interesting to compare our values of the relative errors with the results presented in [25, 26] where the recognition of lattice types was done with the aid of parametric identification methods. By way of example let us look at the best result of structure identification obtained in comparative estimation of Bravais cell parameters and Wigner-Seitz cell volumes (Table 6).

The comparison shows that the use of neural nets makes it possible to significantly decrease the structure identification failure rates for the following lattice types:

—trigonal and cubic types from 26 to 2%;

—orthorhombic and tetragonal types from 34 to 16%;

—tetragonal and cubic types from 26 to 12%;

—orthorhombic and cubic types from 15 to 8%.

On the other hand, when discriminating monoclinic and hexagonal lattices from lattices of subgroups 3 and 4, the neural nets give much worse results than parametric identification methods. Particularly, in separation of hexagonal lattices from tetragonal ones the relative error has grown from 0 to 43%.

As for subgroup 4, here the low results are due to the geometric overlapping of classes. A set of cubic-type lattices (white diagonal in Fig. 5) lie in the same line in the three-dimensional space. This line is in the plane containing tetragonal-type elements (the dark-grey layer in Fig. 5). The plane lies in turn inside the parallelogram formed by orthorhombic-type elements (the light-grey cube in Fig. 5).

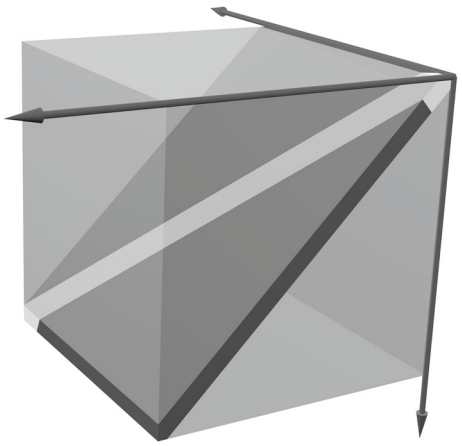

Fig. 5. The class overlapping of lattice types of subgroup 4.

CONCLUSIONS

We have offered a three-stage learning technique for neural networks. Crystal lattices are divided into non-overlapping classes in the first two stages. Crystal lattices belonging to overlapping classes are recognized at the last stage.

The investigation showed that the Mamdani-Zadeh neural net is particularly sensitive to the size of the learning sample and it is necessary to use no less than 1000 lattices of each lattice system type to ensure efficient work.

As compared with parametric identification methods, the use of neural nets makes it possible to decrease the 3D structure identification failure rate for four couples of lattice systems considerably (as much as 2 to 13 times).

The research results allow us to draw a conclusion that fuzzy neural networks are an efficient tool in recognition of crystal lattice types using Bravais cells parameters.

ACKNOWLEDGMENTS

This work was partially supported by the Ministry of education and science of the Russian Federation in the framework of the implementation of the Program of increasing the competitiveness of SSAU among the world's leading scientific and educational centers for 2013–2020 years; by the Russian Foundation for Basic Research grants (# 15-29-03823, # 15-29-07077, # 16-41-630761; # 16-29-11698, # 17-01-00972); by the ONIT RAS program # 6 "Bioinformatics, modern information technologies and mathematical methods in medicine" 2017.

REFERENCES

1. Tilley, R., *Crystals and Crystal Structure*, John Wiley & Sons, 2006, pp. 17–32.
2. Kessler, E.G., Henins, A., Deslattes, R.D., Nielsen, L., and Arif, M., Precision comparison of the lattice parameters of silicon monocrystals, *J. Res. Nat. Inst. Standards Technol.*, 1994, vol. 99, no. 1, pp. 1–18.
3. Smith, W.F., *Foundations of Materials Science and Engineering*, N.Y.: McGraw-Hill, 2004, pp. 67–107.
4. Patera, J. and Skala, V., *Centered cubic lattice method comparison*, *Proc. Algoritmy*, 2005, pp. 309–319.
5. Hammond, C., *The Basic of Crystallography and Diffraction*, 3rd ed., Oxford University Press, 2009, pp. 55–83.
6. Soifer, V.A. and Kupriyanov, A.V., Analysis and recognition of the nanoscale images: Conventional approach and novel problem statement, *Comput. Opt.*, 2011, vol. 35, no. 2, pp. 136–144.
7. Kirsh, D.V. and Kupriyanov, A.V., Parallel implementations of parametric identification algorithms for three-dimensional crystal lattices, *CEUR Workshop Proc.*, 2016, vol. 1638, pp. 451–459.
8. Kupriyanov, A.V. and Kirsh, D.V., Estimating the similarity measure of crystal lattices by coordinates of their nodes in three-dimensional space, *Comput. Opt.*, 2012, vol. 36, no. 4, pp. 590–595.
9. Kupriyanov, A.V., Texture analysis and determination of crystal lattice type using nano-scale patterns, *Comput. Opt.*, 2011, vol. 35, no. 2, pp. 144–151.
10. Lyozina, I.V. and Krasnov, A.E., Fuzzy multilayer perceptron identification properties examination, *Samara Res. Center Bull.*, 2014, vol. 16, no. 4(2), pp. 340–343.
11. Lyozin, I.A. and Markelov, D.E., Investigation of automated design-engineering parts classification system using data bases, *Chief Mech.*, 2014, no. 5, pp. 38–41.
12. Soldatova, O.P., Multifunctional neural network simulator, *Software Software Systems*, 2012, no. 3, pp. 27–31.
13. Soldatova, O.P. and Danilenko, A.N., A hybrid fuzzy neural classifier for handling the classification problem in decision making under fuzzy input conditions, *Samara Res. Center Bull.*, 2014, vol. 16, no. 4(2), pp. 350–358.
14. Soldatova, O.P. and Pudikova, E.M., A hybrid modification of Wang-Mendel neural net used for classifying system error flow, *Samara Res. Center Bull.*, 2014, vol. 16, no. 4(2), pp. 359–390.
15. Vineetha, S., Bhat, C.C.S., and Idicula, S.M., MicroRNA–mRNA interaction network using TSK-type recurrent neural fuzzy network, *Gene*, 2013, vol. 515, no. 2, pp. 385–390.
16. Kiper, A.V. and Stankevich, T.S., Development of a fuzzy classifier using the Sugeno fuzzy system for ranking a fire on the seaport premises, *Astrakhan State Tech. Univ. Bull., Marine Eng. Ser.*, 2012, no. 2, pp. 18–25.
17. Katasyov, S.A., Software for building fuzzy rule Inference data bases for expert systems, *Fundamental Res.*, 2013, no. 10(9), pp. 1922–1927.
18. Osovsky, S., *Data Processing Neural Nets, M.*: Finance and Statistics, 2002, p. 344.
19. Rutkovskaya, D., Pilinsky, M., and Rutkovsky, L., *Neural Nets, Genetic Algorithms and Fuzzy Systems, translated from Polish by Rudinsky, I.D., M.*: Hotline-Telecom, 2006, p. 52.
20. Novak, V., Perfilieva, I., and Mockor, J., Mathematical principles of fuzzy logic, *Kluwer Int. Ser. Eng. Comput. Sci.*, 1999, vol. 517, p. 352.
21. Soldatova, O.P. and Lyozin, I.A., Solving the classification problem using Mamdani-Zadeh system-based fuzzy neural rule inference networks, *Samara Res. Center Bull., Phys. Math. Sci. Ser.*, 2014, vol. 16, no. 2(35), pp. 136–148.
22. Kirsh, D.V. and Kupriyanov, A.V., Modeling and identification of centered crystal lattices in three-dimensional space, *CEUR Workshop Proc.*, 2015, vol. 1490, pp. 162–170.
23. Shirokanev, A.S., Kirsh, D.V., and Kupriyanov, A.V., Application of gradient steepest descent method to the problem of crystal lattice parametric identification, *CEUR Workshop Proc.*, 2016, vol. 1638, pp. 393–400.
24. Andrews, L.C. and Bernstein, H.J., Lattices and reduced cells as points in 6-space and selection of Bravais lattice type by projections, *Foundations Cryst.*, 1988, vol. 44, no. 6, pp. 1009–1018.
25. Kirsh, D.V. and Kupriyanov, A.V., Crystal lattice identification by coordinates of their nodes in three dimensional space, *Pattern Recognit. Image Anal.*, 2015, vol. 25, no. 3, pp. 456–460.
26. Kirsh, D.V. and Kupriyanov, A.V., Identification of three-dimensional crystal lattices by estimation of their unit cell parameters, *Supplementary Proceedings of the 4th International Conference on Analysis of Images, Social Networks and Texts (AIST'2015)*, 2015, pp. 40–45.